NANO LETTERS

pubs.acs.org/NanoLett Letter

Enhanced Heat Dissipation in Gallium Nitride-Based Light-Emitting Diodes by Piezo-phototronic Effect

Qi Guo,[⊥] Ding Li,[⊥] Qilin Hua, Keyu Ji, Wenhong Sun,* Weiguo Hu,* and Zhong Lin Wang*

Cite This: https://doi.org/10.1021/acs.nanolett.1c00999 Read Online

ACCESS | Metrics & More | Article Recommendations

ABSTRACT: As a new generation of light sources, GaN-based light-emitting diodes (LEDs) have wide applications in lighting and display. Heat dissipation in LEDs is a fundamental issue that leads to a decrease in light output, a shortened lifespan, and the risk of catastrophic failure. Here, the temperature spatial distribution of the LEDs is revealed by using high-resolution infrared thermography, and the piezo-phototronic effect is proved to restrain efficaciously the temperature increment for the first time. We observe the temperature field and current density distribution of the LED array under external strain compensation. Specifically, the temperature rise caused by the self-heating effect is reduced by 47.62% under 0.1% external strain, which is attributed to the enhanced competitiveness of radiative recombination against nonradiative recombination due to the piezo-phototronic effect. This work not only deepens the understanding of the piezo-phototronic effect in LEDs but also provides a novel, easy-to-implement, and economical method to effectively enhance thermal management.

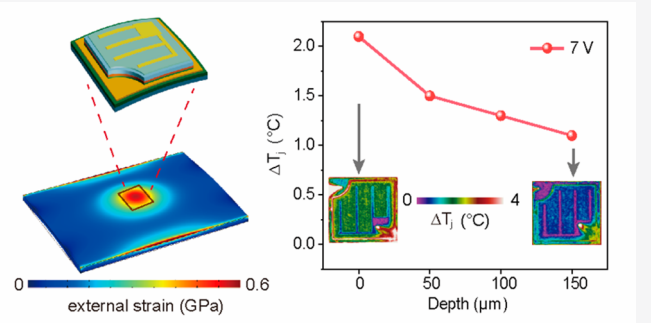

KEYWORDS: *GaN-based LEDs, self-heating effect, thermal management, infrared thermography, piezo-phototronic effect*

Light-emitting diodes (LEDs) have acquired rapid developments in the past decades with applications widely existing in the fields of general lighting,[1] traffic signals,[2] digital displays,[3] biomedical treatments,[4,5] etc. High-power light-emitting diodes (HPLEDs) have been considered as one of the most important development directions for nitride semiconductors.[6−8] However, heat dissipation is the most significant problem that hinders the application of HPLEDs in the field of high power and high brightness.[9−12] Due to the self-heating effect, that is, the internal heat generated when a large current is injected, the internal quantum efficiency (IQE) and external quantum efficiency (EQE) of the LEDs are significantly reduced,[13−15] which degrades the luminous performance and service life of the HPLED. Similarly, GaN-based micro-LEDs also have to face serious heat dissipation and thermal management issues. The flexible plastic substrate of the micro-LED has low thermal conductivity,[16,17] which would prevent heat dissipation and enhance the self-heating effect, thereby reducing the luminous intensity and quantum efficiency. Moreover, due to the small size, large number, and high integration of micro-LEDs,[3,18] it is still a challenge to solve the heat dissipation problem of micro-LEDs on a thermally and electrically insulated plastic substrate. Therefore, the thermal management of LEDs is very critical for addressing the heat dissipation issue. Traditional thermal management methods include active and passive thermal designs, such as heat pipes and vapor chambers,[19] heat sinks,[20,21] flip-chip packaging,[22] thermoelectric devices,[23] liquid cooling systems,[24,25] etc. However, these thermal management designs are usually huge in size, complex in structure, and high cost and therefore are facing more and more restrictions. It is expected that there will be some kind of thermal management technology that is easy to manufacture and is operable and economical.

In this work, we proposed a new method to adjust the self-heating effect of HPLED through external strain. According to the piezo-phototronic effect, the piezoelectric polarization charge generated by the external strain can significantly modulate the energy band profile of the GaN-based HPLED, thereby greatly regulating the electron−hole radiative and nonradiative recombination rate, and finally adjust the self-heating effect mainly produced by nonradiative recombination. The piezo-phototronic effect has been widely used to regulate the performance of biological/chemical sensors,[26−28] pressure imaging,[29] Boolean logic,[30,31] electronic skins,[32] photovoltaic devices,[33,34] optoelectronic devices,[35,36] etc. However, the

Received: March 11, 2021
Revised: April 17, 2021

https://doi.org/10.1021/acs.nanolett.1c00999
Nano Lett. XXXX, XXX, XXX−XXX

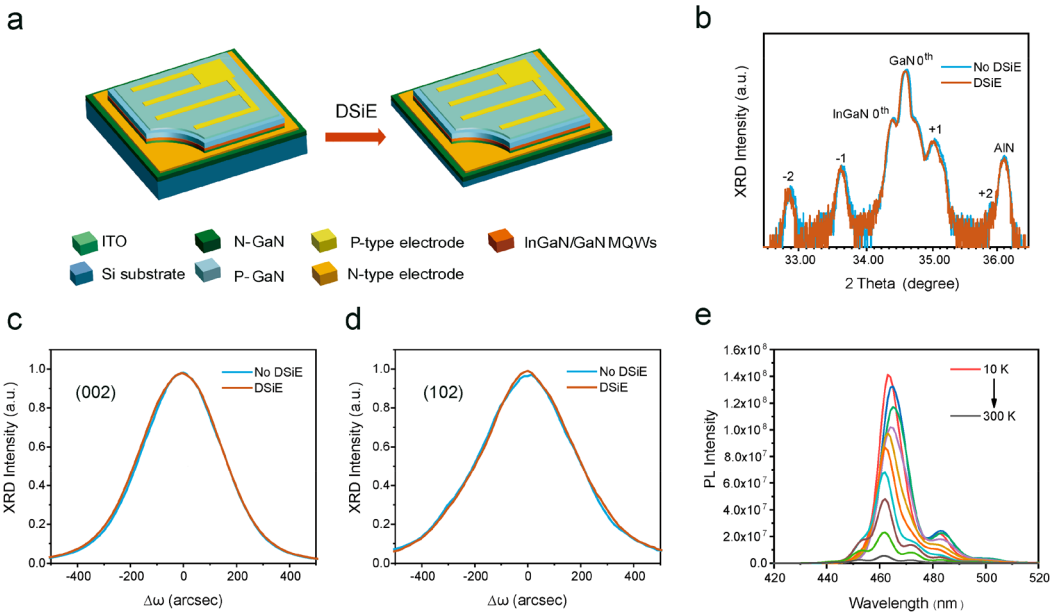

Figure 1. Optical and crystal properties of $In_{0.16}Ga_{0.84}N$/GaN MQWs LEDs before and after DSiE. (a) Schematic diagram of LED device before and after DSiE. High-resolution XRD: (b) 2θ-ω scans, (c) symmetric (002), and (d) asymmetric (102) ω-scan rocking curves. (e) PL spectra under various temperatures from 10 to 300 K.

modulation of the piezo-phototronic effect on the self-heating effect in LEDs has not been reported until now.

Here, we have fabricated the high-power InGaN/GaN multiple quantum wells (MQWs) blue-LED with 2 × 2 mm^2 active region, and have demonstrated the self-heating effect modulation realized by the piezo-phototronic effect for the first time. The in-plane distribution of injected current and junction temperature has been visualized by the infrared thermography under various strains. When external strain was applied, it can effectively improve radiative recombination efficiency and reduce the self-heating effect. Under the condition of strain compensation, the self-heating temperature of the LED at 7 V bias voltage has been reduced by 47.62% compared with the traditional strain-free LED device. This work clearly reveals the mechanism by which the piezo-phototronic effect modulates the current injection, carrier recombination, and self-heating effect in the LEDs, which provides a novel solution to solve the heat dissipation and thermal management problems of the HPLED lighting and displays.

Results and Discussion. The arrays of high-power $In_{0.16}Ga_{0.84}N$/GaN MQWs LEDs were successfully fabricated by using the micro-nano fabrication technology. The light-emitting area of a single device is 2 × 2 mm^2, which is about 4 times larger than common 45 mil LED chips. The $In_{0.16}Ga_{0.84}N$/GaN MQWs were grown on a 1.5 mm-thick silicon substrate via metal−organic chemical vapor deposition. Figure 1a illustrates the schematic diagram of the $In_{0.16}Ga_{0.84}N$/GaN MQWs LEDs. From top to bottom, the epitaxial structure on Si substrate is 0.2 μm-thick Mg-doped p-GaN layer (including a 40 nm-thick AlGaN electron blocking layer), 10-period InGaN (3 nm)/GaN (7 nm) MQWs, 2 μm-thick Si-doped n-GaN layer, 0.6 μm-thick undoped GaN layer, and 1 μm-thick AlN and AlGaN buffer layers. We also sputtered the indium tin oxide (ITO) thin film as the current spreading layer for its high optical transparency and electrical conductivity.

In order to easily introduce external strain, we carried out the deep silicon etching process (DSiE) to thin the silicon substrate, as shown in Figure 1a. Furthermore, we conducted high-resolution X-ray diffraction (XRD) measurements to characterize the crystal quality of the LED before and after DSiE,[37] and the results are shown in Figure 1b−d. Figure 1b exhibits sharp peaks of GaN 0^{th} and InGaN 0^{th} and the periodic satellite peaks (from −2 to +2), which shows smooth interfaces of $In_{0.16}Ga_{0.84}N$/GaN multiple quantum well. The GaN 0^{th} and InGaN 0^{th} shifted slightly to the left after the silicon substrate is etched to about 500 μm, which indicates a slight decrease of the in-plane residual tensile strain in the material. The full width at half-maximum (FWHM) of the rocking curve in the ω scans mode reveals the dislocation density.[38] It is clearly shown in Figure 1c that the FWHM of the GaN (002) plane on the silicon substrate is 354.686 arcsec before DSiE and slightly increases to 364.578 arcsec after DSiE. Similarly, the FWHM of the rocking curve of (102) GaN 0^{th} slightly increases from 406.976 arcsec to 419.827 arcsec after DSiE, as shown in Figure 1d. These results indicate that the thinning of the silicon substrate by DSiE hardly damages the crystal quality of the LED device. Figure 1e shows the photoluminescence (PL) spectra of the InGaN/GaN MQWs structure (without external strain) as a function of temperature. As the temperature drops from 300 K to 10K, the radiative recombination gradually dominates, thereby increasing the PL intensity. The emission peak shift shows a classic S-shape with the increase of temperature, which is commonly connected to a transformation in the carrier dynamics with the increasing temperature due to inhomogeneity and carrier localization in the InGaN/GaN MQWs.[39]

To further reveal the modulation characteristics of the piezo-phototronic effect on the performance of the LEDs, the influence of external strain on the lattice strain of InGaN and GaN layers is characterized. Since micro-Raman spectroscopy can evaluate the residual stress in InGaN/GaN MQWs,[40] we conducted the Raman spectra measurements on InGaN/GaN

https://doi.org/10.1021/acs.nanolett.1c00999
Nano Lett. XXXX, XXX, XXX−XXX

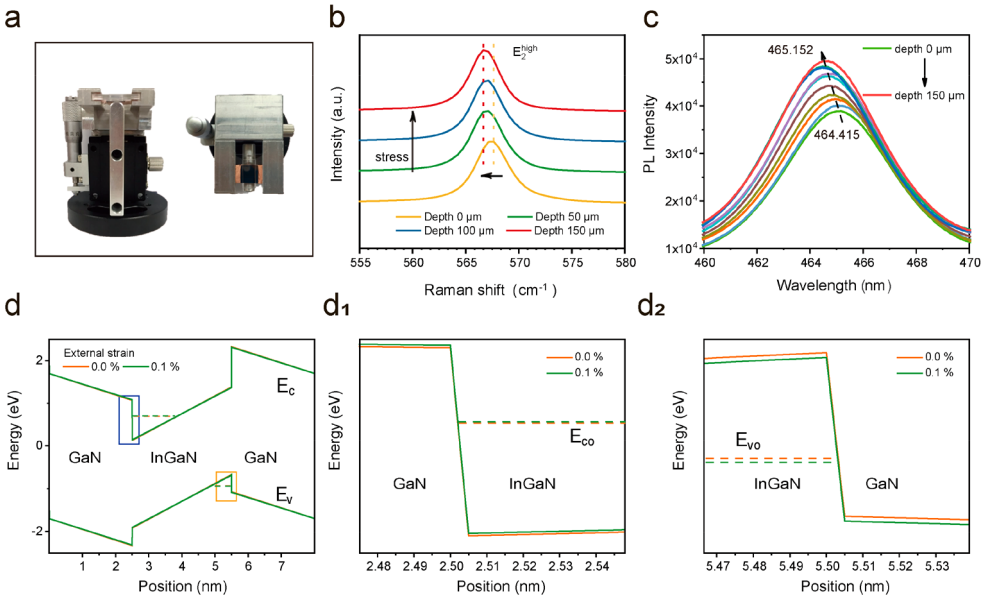

Figure 2. Modulation mechanism of the piezo-phototronic effect in the $In_{0.16}Ga_{0.84}N$/GaN MQWs LEDs. (a) Pictures of customized strain control setup, and magnitude of the external force is expressed in terms of the precession depth. (b) Micro-Raman spectra under various external strains. (c) PL spectra under various external strains. (d) Corresponding energy band profiles and ground state energy level of the conduction band (E_{C0}) and valence band (E_{V0}) in GaN/InGaN quantum well. (d_1) The enlarged conduction band and E_{C0} labeled by blue rectangular box. (d_2) The enlarged valence band and E_{V0} labeled by orange rectangular box.

MQWs LEDs under different external strains. The customized experimental setup shown in Figure 2a can apply different external strains to the LED chips, and the rising distance of the knob reflects the different external strains applied to the sample. Because the Raman E_2^{high} phonon mode peak of GaN is sensitive to the stress state,[41] the residual stress change can be estimated by observing the relative movement of E_2^{high}. According to the biaxial strain model (eq 1):[41,42]

$$\sigma_{xx} = \frac{\Delta\omega_{P_h}}{K_{P_h}^{biax}} \quad (1)$$

where σ_{xx} is residual stress, $\Delta\omega_{P_h} = \omega - \omega_0$, ω is the measured peak position, ω_0 is 568 cm^{-1}[43] as the standard value for bulk GaN, and $K_{P_h}^{biax}$ is the biaxial stress coefficient. The detailed behavior of the phonon mode peaks of GaN E_2^{high} under different strains is shown in Figure 2b. It can be found that, as the precession depth increases from 0 to 150 μm, the frequency value of the E_2^{high} mode decreases from 567.63 to 566.66 cm^{-1}, and the residual stress of the GaN layer increases significantly from 0.14 to 0.52 GPa. According to the linear elasticity theory,[40,44] the external strain applied to the GaN layer increases from 0.0% to 0.1%. Since the lattice constant of GaN is smaller than that of InGaN, the InGaN layer in the LED quantum wells bears the in-plane compressive strain from the GaN layer. As the in-plane tensile strain in the GaN layer increases, the in-plane compressive strain in the InGaN layer is getting smaller in the quantum wells,[45] which represents the external strain partly compensates for the internal strain caused by the lattice mismatch.

The PL measurement has also been performed on InGaN/GaN MQWs LEDs to study the emission densities under different strains. The main emission of the LED is typically identified as the transition of the electron from the ground-state energy level of conduction band to the ground-state energy level of valence band. As illustrated in Figure 2c, the dominant peak located at 464.415 nm is observed for the InGaN/GaN MQWs LEDs without external strain, and a slight blue shift of the emission peak occurs as the externally applied strain in the GaN layer increases from 0.0% to 0.1%. Simultaneously, the emission intensity of PL increases significantly by 26.6% under an external strain of 0.1%. This experimental phenomenon can be further explained by the physical principle of piezo-phototronic effect. Due to the noncentrosymmetric crystal structure of wurtzite group III nitride materials, there are spontaneous polarization charges on the surface of the material. Meanwhile, the lattice mismatch between InGaN and GaN films also induces piezoelectric polarization charges at the interface. In the absence of external strain, the net polarization charge at the InGaN/GaN interface causes the quantum wells energy band tilt, which leads to the electron wave function and hole wave function separated in opposite directions in the wells, thereby weakening the radiative recombination. This phenomenon is known as the quantum-confined Stark effect.[46] However, under the external strain along the *c*-axis, the piezoelectric polarization charges of the InGaN layer are counteracted partly, and the potential well in the InGaN layer tends to the flat-band condition. Consequently, the overlap of the electron−hole wave functions is enhanced, and the radiative recombination rate is greatly increased.

In order to verify our experimental results and reveal the in-depth modulation mechanism of the piezo-phototronic effect on the photoelectric characteristics of the InGaN/GaN MQWs LEDs, we calculated the energy band and ground-state energy level of InGaN/GaN quantum well under different strains based on the Poisson−Schrödinger self-consistent calculation and piezoelectric constitutive equation, as shown in Figure 2d. Without external strain applied, the transition energy between the ground-state energy level of the conduction band (E_{C0}) and the valence band (E_{V0}) is about 1.6322 eV. When an external strain of 0.1% is applied, the reduction of the in-plane

https://doi.org/10.1021/acs.nanolett.1c00999
Nano Lett. XXXX, XXX, XXX−XXX

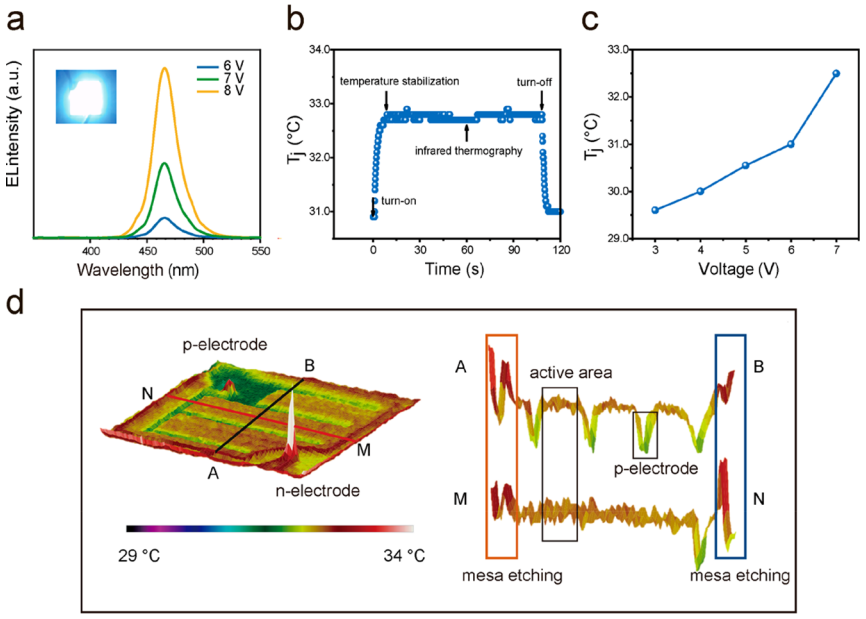

Figure 3. Self-heating effect of LED devices. (a) EL spectra of LED measured under different applied voltage. (b) The junction temperature (T_j) as a function of time and (c) applied voltage. (d) Infrared thermography showing the junction temperature (T_j) of different areas at 7 V bias voltage as well as a partial enlarged view.

strain experienced by the InGaN layer modulates the piezoelectric polarization charges and causes the energy band at the InGaN/GaN quantum well to flatten. In addition, the ground-state energy level of the conduction band E_{C0} increases, while the ground-state energy level of the valence band E_{V0} decreases (Figure 2d$_1$,d$_2$). The transition energy slightly increases to 1.6478 eV, which in turn leads to the blue shift of the PL emission peak. Therefore, it is proved that the external strain makes the quantum well energy band tilt smaller, which enhances the overlap of the electron−hole wave function and greatly increases the radiative recombination rate. This mechanism has also been discussed theoretically and experimentally in the previous papers.[47−49]

The electroluminescence (EL) spectra of LEDs without external strain under different applied voltages are illustrated in Figure 3a. The EL peaks at around 465 nm correspond to near-band edge luminescence. The FWHM of the EL spectrum is 22 nm at 7 V bias voltage. A camera image of the blue LED emission is shown in the inset, which was taken at 7 V bias voltage. Furthermore, in order to characterize the self-heating effect of the LEDs, a noncontact emerging high-resolution infrared thermography method is used to visualize the thermal distribution and indirectly reflect the injected current distribution of the LEDs.[50] Based on the thermal analysis of the LEDs, junction temperature (T_j) is a physical quantity commonly used to evaluate heat.[51] Since the heat dissipation conditions of the entire area remain unchanged in the p−n junction, the junction temperature only depends on the heat released by nonradiative recombination. Figure 3b represents the time dependence of the T_j in the LED chip under a constant applied voltage. The T_j rises quickly in 10 s after a 7 V bias voltage is applied and then reaches a relatively stable value of 32.7 ± 0.1 °C. When the applied bias voltage is removed, T_j quickly drops to the temperature before the LED is turned on within 10 s. Meanwhile, aiming to more accurately evaluate the thermal characteristics of the LED devices, the following discussion of temperature is to select the stable temperature under 60 s injection time as the data collection point. It should be pointed out that the LED chips are directly exposed to the atmosphere without any package. Therefore, this temperature is remarkably lower than the commercial HPLEDs. Figure 3c illustrates the relationship between T_j and applied voltage of the studied LEDs, and T_j quasi-linearity increases with the increase of applied voltage. Similar phenomena have been reported in the previous papers.[51−53]

Figure 3d shows the infrared thermography of the LED chip without external strain, which visually characterizes the junction temperature T_j of different areas when the device is working. Obvious peak temperatures can be clearly observed at n-type contacts (43.2 °C) and p-type contacts (34.0 °C), which are caused by local current crowding. The reason for this phenomenon is that part of the injected carriers are still confined underneath the thick metal pad in contact with the probe, even with a transparent ITO current spreading layer. It can be seen from the 3D partial enlargement on the left of Figure 3d that the temperature of the n-electrode mesa obviously exceeds the temperature of the active region. On the one hand, this is because the hole mobility is much smaller than the electron mobility, resulting in a larger electron−hole density difference at the periphery of the mesa. In turn, the radiative recombination rate in the peripheral area is reduced, and nonradiative recombination heat production is increased.[54−57] On the other hand, the rise in the density of surface defects caused by dry etching also can lead to an increase in nonradiative recombination in the sidewall of the mesa.[58] The temperature of the metal electrode measured in Figure 3d is lower than the actual temperature because the emissivity of the metal electrode (alloy is usually <0.2) is much lower than the emission of semiconductor materials (0.8−0.9) in the far-infrared region of 8−14 μm. We can conclude that the LED chip will generate a lot of heat when it is working, and the temperature of the active region and the electrode will increase accordingly, which will affect the working life and

https://doi.org/10.1021/acs.nanolett.1c00999
Nano Lett. XXXX, XXX, XXX−XXX

reliability of LEDs. Therefore, reducing the self-heating effect is of great significance to the LEDs.

For the first time, we reveal that the piezo-phototronic effect can significantly suppress the self-heating effect of LED devices. We define temperature rise ΔT_j as the difference between the junction temperature (T_j) and the ambient temperature (T_a) during device operation. In the steady-state experiment, since the thermal resistance of the same device is constant, ΔT_j can be used to represent the heat generated (P_h) by the self-heating effect. Figure 4a,b shows infrared thermal imaging of temperature rise ΔT_j without and with external strain in almost the same experimental condition, from which we can see that the ΔT_j of the latter is significantly lower than that of the former. Comparing Figure 4a,b, the ΔT_j of the active region has been significantly reduced from 2.2 to 1.2 °C overall. When the same constant voltage applied, the ΔT_j of the p-type interdigital electrode on the active region also drops by 0.7 °C after external strain modulation, as shown in the 3D partial enlarged view. The reduction in ΔT_j illustrates the decrease in the junction temperature of the active region and p-type electrode. Moreover, the ΔT_j of the p-GaN step is reduced from 3.6 to 2.5 °C under strain compensation condition, which indicates that the sidewall temperature rise of the p-type step has also been significantly suppressed. Because the junction temperature mainly depends on the heat generated by nonradiative recombination, we can attribute the drop in ΔT_j to the decrease in nonradiative recombination. Figure 4c manifests the current−voltage ($I-V$) characteristics of the LED measured under various strains. With increasing external strain, the $I-V$ curves very slightly title up. The turn-on current value increased slightly by 0.07 mA under the external strain 0.1%. This can be explained by the simplified theory of Shockley. The recombination current is inversely proportional to the carrier lifetime, which decreases as the external strain increases.[59] Figure 4e illustrates the relationship between ΔT_j and external strain at 6 and 7 V bias voltages. It clearly shows that the ΔT_j has a significant decrease when the external strain increases at both 6 and 7 V bias voltages, which indicates that the self-heating effect of LED has been greatly suppressed. The decreased self-heating effect can be defined as $(\Delta T_{j_1} - \Delta T_{j_0})/\Delta T_{j_0}$, where ΔT_{j_1} and ΔT_{j_0} are the temperature rise with and without external strain, respectively. It can be clearly seen that the piezo-phototronic effect under the maximum external strain reduces the self-heating effect by 50% and 47.62% at 6 and 7 V bias voltages, respectively. The piezo-phototronic effect has been proven to effectively suppress the self-heating effect of InGaN/GaN MQWs LEDs.

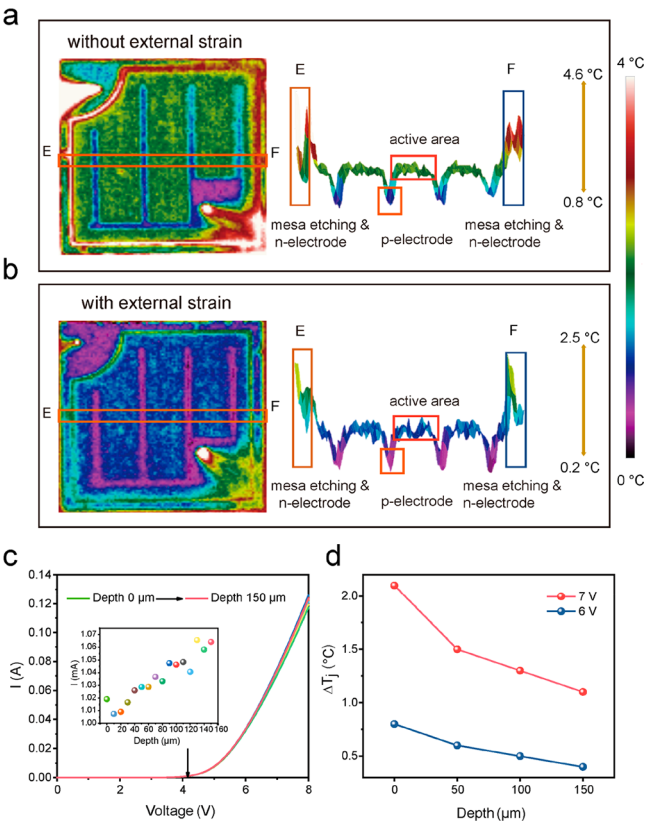

Figure 4. Piezo-phototronic effect modulated self-heating effect in LEDs. Infrared thermography showing the temperature rise ΔT_j of different areas at 7 V bias voltage (a) without external strain and (b) with external strain. (c) $I-V$ curve under different strain control, and the current under different strains at 4 V bias voltage. (d) The relationship between temperature rise ΔT_j and external strains at 6 and 7 V bias voltages.

Our experiments have verified that the piezo-phototronic effect can significantly reduce the self-heating effect in the LEDs, and we further elaborate on the physical principles behind this mechanism. The self-heating effect of the LEDs under forwarding current is defined by eq 2a:[59]

$$P_h(T_j) = I_f \times V_f(T_j) - \Phi(T_j) \tag{2a}$$

where P_h is the heat dissipation [W], V_f is the forward voltage [V], and I_f is the forward current [A]. The optical output power is the radiant flux $\Phi(T_j)$. The radiant flux is proportional to the EQE under a constant forward current, which can be expressed as[60,61]

$$\Phi(T_j) \propto \eta_i \eta_{IQE} \tag{2b}$$

where η_{IQE} is the internal quantum efficiency (IQE), and η_i is the optical efficiency; η_i is affected by the LED chip material and refractive index[62] and is a constant during the experiment. Therefore, the self-heating temperature mainly depends on the internal quantum efficiency η_{IQE}. According to the typical ABC model in LEDs,[63] the Shockley−Read−Hall (SRH), radiative, and Auger recombination can be simplified to be AN, BN^2, and CN^3, respectively. The internal quantum efficiency η_{IQE} can be expressed by eq 2c:

$$\eta_{IQE} = \frac{BN^2}{AN + BN^2 + CN^3} \tag{2c}$$

where A, B, and C denote the coefficient for SRH, radiative, and Auger recombination, respectively, and N represents the carrier concentration which depends on the electrical injection efficiency.[64] The radiative coefficient (B) is proportional to the square of the matrix element of the electron−photon coupling Hamiltonian between the electron and hole wave functions, which can be calculated according to the following equations:

$$B = B_0 |\Gamma_{cv}^{mn}|^2 \tag{2d}$$

Γ_{cv}^{mn} is the integral of the electron−hole wave function and can be expressed by eq 2e:

$$\Gamma_{cv}^{mn} = \int dz (\psi_c^m(z))^* \psi_v^n(z) \tag{2e}$$

https://doi.org/10.1021/acs.nanolett.1c00999
Nano Lett. XXXX, XXX, XXX−XXX

where Ψ_c^m and Ψ_v^n is the electron and hole wave functions, respectively. Therefore, the radiative coefficient (B) is proportional to the overlap squared of the electron−hole wave function. In the absence of external strain, due to the combined effects of the spontaneous polarization charges and the piezoelectric polarization charges at the InGaN/GaN interface, the energy band of the InGaN quantum well is tilted, which reduces the overlap of the electron−hole wave function and weakens the radiative recombination rate. When external strain is applied, the piezoelectric polarization charges of the InGaN layer are counteracted partly, thereby flattening the energy band and increasing the wave function overlap integral of electron−hole pairs ($|\Gamma_{cv}^{mn}|^2$).[49] As a consequence, the radiative recombination rate is greatly increased. According to the formula (eq 2a), when the radiant flux ($\Phi(T_j)$) of the LED chip increases, the heat generation ($P_h(T_j)$) will decrease. In our experiments, the piezo-phototronic effect enhances the luminous intensity of PL by 26.6% under the external strain of 0.1%, and the self-heating effect of the LED chip is reduced by 47.62% at 7 V bias voltage, simultaneously. Therefore, the piezo-phototronic effect greatly increases the rate of radiative recombination, thereby promoting the competition of radiative recombination on nonradiative recombination and weakening the self-heating effect. The application of piezo-phototronic effect to suppress the self-heating effect of LEDs is a novel and simple way that can provide economical solutions to the heat dissipation and thermal management of high-brightness HPLED and micro-LED displays.

Conclusions. In summary, the piezo-phototronic effect is proved to enhance the radiative recombination and suppress the self-heating effect of LED devices. Compared with traditional strain-free LEDs, the operating temperature of LEDs under 0.1% applied external strain is reduced by 50.00% and 47.62% at 6 and 7 V bias voltages, respectively. Furthermore, the physical mechanism by which external strain decreases the self-heating effect of LEDs is discussed. By introducing external strain to adjust the piezoelectric polarization charge at the interface, the energy band of the LEDs quantum well and the carrier recombination process can be effectively modulated, thereby dramatically enhancing the competitiveness of radiative recombination against nonradiative recombination and finally decreasing the self-heating effect of the LEDs. This work deepens the understanding of the piezo-phototronic effect in nitride-based LEDs and proposes a systematic method to suppress the self-heating effect of LEDs through external strain, which has cutting-edge scientific value and broad application prospects.

Methods. *Fabrication of InGaN/GaN MQWs LEDs.* First, we fabricated the mesa area of each device by photolithography and ICP etching technology and then deposited the Ti/Al/Ni/Au (20 nm/120 nm/45 nm/55 nm) multilayer metal on the exposed N-type GaN layer by electron beam evaporation. It was annealed at 800 °C for 30 s in the N_2 atmosphere to prepare an n-electrode with good Ohmic contact. As a good current diffusion layer, ITO thin film has high transparency in the visible spectrum, and its good conductivity is convenient for collecting current. Therefore, before making the p-electrode, we first sputtered the ITO layer by RF magnetron sputter and then annealed it in the air at 550 °C for 10 min. Finally, we sputtered the Ni/Au (30/150 nm) onto the sample surface by magnetron sputter as the p-electrode and annealed it at 500 °C for 2 min in the N_2 atmosphere.

Optical, Electrical, and Thermal Characterizations. The XRD measurement was performed using the Bruker D8 system. The experiment used FLS980-S2S2-STM equipment (xenon lamp as the excitation source) for temperature-dependent PL and precise low-temperature control through liquid helium. The Raman measurement with 532 nm laser and PL with 325 nm laser under different strains were performed with a micro-Raman spectrometer (LabRAM HR Evolution) at room temperature. The infrared band of the microscopic infrared hot spot location measurement system (GMARG-A4) is 8−14 μm, and the image resolution is about 5 μm. The $I-V$ characteristics are measured using a Keithley 2450 source meter.

AUTHOR INFORMATION

Corresponding Authors

Wenhong Sun − *Research Center for Optoelectronic Materials and Devices, School of Physical Science and Technology, Guangxi University, Nanning 530004, China*; Email: 20180001@gxu.edu.cn

Weiguo Hu − *Center on Nanoenergy Research, School of Physical Science and Technology, Guangxi University, Nanning, Guangxi 530004, P.R. China; CAS Center for Excellence in Nanoscience, Beijing Key Laboratory of Micro-nano Energy and Sensor, Beijing Institute of Nanoenergy and Nanosystems, Chinese Academy of Sciences, Beijing 101400, P.R. China; School of Nanoscience and Technology, University of Chinese Academy of Sciences, Beijing 100049, P.R. China*; orcid.org/0000-0002-8614-0359; Email: huweiguo@binn.cas.cn

Zhong Lin Wang − *Center on Nanoenergy Research, School of Physical Science and Technology, Guangxi University, Nanning, Guangxi 530004, P.R. China; CAS Center for Excellence in Nanoscience, Beijing Key Laboratory of Micro-nano Energy and Sensor, Beijing Institute of Nanoenergy and Nanosystems, Chinese Academy of Sciences, Beijing 101400, P.R. China; School of Nanoscience and Technology, University of Chinese Academy of Sciences, Beijing 100049, P.R. China*; orcid.org/0000-0002-5530-0380; Email: zlwang@gatech.edu

Authors

Qi Guo − *Center on Nanoenergy Research, School of Physical Science and Technology, Guangxi University, Nanning, Guangxi 530004, P.R. China; CAS Center for Excellence in Nanoscience, Beijing Key Laboratory of Micro-nano Energy and Sensor, Beijing Institute of Nanoenergy and Nanosystems, Chinese Academy of Sciences, Beijing 101400, P.R. China; School of Nanoscience and Technology, University of Chinese Academy of Sciences, Beijing 100049, P.R. China; Research Center for Optoelectronic Materials and Devices, School of Physical Science and Technology, Guangxi University, Nanning 530004, China*; orcid.org/0000-0001-9700-1568

Ding Li − *CAS Center for Excellence in Nanoscience, Beijing Key Laboratory of Micro-nano Energy and Sensor, Beijing Institute of Nanoenergy and Nanosystems, Chinese Academy of Sciences, Beijing 101400, P.R. China; School of Nanoscience and Technology, University of Chinese Academy of Sciences, Beijing 100049, P.R. China*

Qilin Hua − *CAS Center for Excellence in Nanoscience, Beijing Key Laboratory of Micro-nano Energy and Sensor, Beijing Institute of Nanoenergy and Nanosystems, Chinese Academy*

https://doi.org/10.1021/acs.nanolett.1c00999
Nano Lett. XXXX, XXX, XXX−XXX

of Sciences, Beijing 101400, P.R. China; School of Nanoscience and Technology, University of Chinese Academy of Sciences, Beijing 100049, P.R. China; orcid.org/0000-0002-5269-5532

Keyu Ji − *Center on Nanoenergy Research, School of Physical Science and Technology, Guangxi University, Nanning, Guangxi 530004, P.R. China; CAS Center for Excellence in Nanoscience, Beijing Key Laboratory of Micro-nano Energy and Sensor, Beijing Institute of Nanoenergy and Nanosystems, Chinese Academy of Sciences, Beijing 101400, P.R. China; School of Nanoscience and Technology, University of Chinese Academy of Sciences, Beijing 100049, P.R. China; Research Center for Optoelectronic Materials and Devices, School of Physical Science and Technology, Guangxi University, Nanning 530004, China*

Complete contact information is available at: https://pubs.acs.org/10.1021/acs.nanolett.1c00999

Author Contributions

⊥These authors contributed equally to this work.

Notes

The authors declare no competing financial interest.

■ ACKNOWLEDGMENTS

The authors thank for the support from the National Key Research and Development Program of China (2016YFA0202703), the National Natural Science Foundation of China (61904012), the Natural Science Foundation of Beijing Municipality (4204114), Bagui Talent of Guangxi Province (T3120097921 and T31200992001), and Talent Model Base Program (AD19110157).

■ REFERENCES

(1) Waltereit, P.; Brandt, O.; Trampert, A.; Grahn, H. T.; Menniger, J.; Ramsteiner, M.; Reiche, M.; Ploog, K. H. Nitride semiconductors free of electrostatic fields for efficient white light-emitting diodes. *Nature* **2000**, *406* (6798), 865−8.

(2) Firdous, A.; Indu; Niranjan, V. Smart Density Based Traffic Light System. Proceedings from the *8th International Conference on Reliability, Infocom Technologies and Optimization (Trends and Future Directions) (ICRITO)*, 4−5 June 2020, Noida, India; IEEE: New York; pp 497−500.

(3) Huang, Y.; Hsiang, E. L.; Deng, M. Y.; Wu, S. T. Mini-LED, Micro-LED and OLED displays: present status and future perspectives. *Light: Sci. Appl.* **2020**, *9* (1), 105.

(4) Sha, W.; Zhang, J. C.; Tan, S. X.; Luo, X. D.; Hu, W. G. III-nitride piezotronic/piezo-phototronic materials and devices. *J. Phys. D: Appl. Phys.* **2019**, *52* (21), 213003.

(5) Nimbalkar, M.; Yawalkar, M.; Mahajan, N.; Dhoble, S. J. Potential of luminescent materials in phototherapy. *Photodiagn. Photodyn. Ther.* **2021**, *33*, 102082.

(6) Zhao, C.; Ng, T. K.; ElAfandy, R. T.; Prabaswara, A.; Consiglio, G. B.; Ajia, I. A.; Roqan, I. S.; Janjua, B.; Shen, C.; Eid, J.; Alyamani, A. Y.; El-Desouki, M. M.; Ooi, B. S. Droop-Free, Reliable, and High-Power InGaN/GaN Nanowire Light-Emitting Diodes for Monolithic Metal-Optoelectronics. *Nano Lett.* **2016**, *16* (7), 4616−23.

(7) Piprek, J. Comparative analysis of efficiency limitations in GaN-based blue laser diodes. Proceedings from the *2016 International Conference on Numerical Simulation of Optoelectronic Devices (NUSOD)*, July 11−15, 2016, Sydney, Australia; IEEE: New York, 2016; pp 205−206.

(8) Harbers, G.; Bierhuizen, S. J.; Krames, M. R. Performance of high power light emitting diodes in display illumination applications. *J. Disp. Technol.* **2007**, *3* (2), 98−109.

(9) Kim, M. H.; Schubert, M. F.; Dai, Q.; Kim, J. K.; Schubert, E. F.; Piprek, J.; Park, Y. Origin of efficiency droop in GaN-based light-emitting diodes. *Appl. Phys. Lett.* **2007**, *91* (18), 183507.

(10) Efremov, A. A.; Bochkareva, N. I.; Gorbunov, R. I.; Lavrinovich, D. A.; Rebane, Y. T.; Tarkhin, D. V.; Shreter, Y. G. Effect of the Joule heating on the quantum efficiency and choice of thermal conditions for high-power blue InGaN/GaN LEDs. *Semiconductors* **2006**, *40* (5), 605−610.

(11) Han, N.; Cuong, T. V.; Han, M.; Ryu, B. D.; Chandramohan, S.; Park, J. B.; Kang, J. H.; Park, Y. J.; Ko, K. B.; Kim, H. Y.; Kim, H. K.; Ryu, J. H.; Katharria, Y. S.; Choi, C. J.; Hong, C. H. Improved heat dissipation in gallium nitride light-emitting diodes with embedded graphene oxide pattern. *Nat. Commun.* **2013**, *4*, 1452.

(12) Du, C. H.; Jing, L.; Jiang, C. Y.; Liu, T.; Pu, X.; Sun, J. M.; Li, D. B.; Hu, W. G. An effective approach to alleviating the thermal effect in microstripe array-LEDs via the piezo-phototronic effect. *Mater. Horiz.* **2018**, *5* (1), 116−122.

(13) Schubert, M. F.; Xu, J.; Kim, J. K.; Schubert, E. F.; Kim, M. H.; Yoon, S.; Lee, S. M.; Sone, C.; Sakong, T.; Park, Y. Polarization-matched GaInN/AlGaInN multi-quantum-well light-emitting diodes with reduced efficiency droop. *Appl. Phys. Lett.* **2008**, *93* (4), 041102.

(14) Nippert, F.; Karpov, S. Y.; Callsen, G.; Galler, B.; Kure, T.; Nenstiel, C.; Wagner, M. R.; Strassburg, M.; Lugauer, H. J.; Hoffmann, A. Temperature-dependent recombination coefficients in InGaN light-emitting diodes: Hole localization, Auger processes, and the green gap. *Appl. Phys. Lett.* **2016**, *109* (16), 161103.

(15) Zhao, L. N.; Yan, D. W.; Zhang, Z. H.; Hua, B.; Yang, G. F.; Cao, Y. R.; Zhang, E. X.; Gu, X. F.; Fleetwood, D. M. Temperature-Dependent Efficiency Droop in GaN-Based Blue LEDs. *IEEE Electron Device Lett.* **2018**, *39* (4), 528−531.

(16) Moe, C. G.; Reed, M. L.; Garrett, G. A.; Sampath, A. V.; Alexander, T.; Shen, H.; Wraback, M.; Bilenko, Y.; Shatalov, M.; Yang, J.; Sun, W.; Deng, J.; Gaska, R. Current-induced degradation of high performance deep ultraviolet light emitting diodes. *Appl. Phys. Lett.* **2010**, *96* (21), 213512.

(17) Chun, J.; Hwang, Y.; Choi, Y.-S.; Kim, J.-J.; Jeong, T.; Baek, J. H.; Ko, H. C.; Park, S.-J. Laser lift-off transfer printing of patterned GaN light-emitting diodes from sapphire to flexible substrates using a Cr/Au laser blocking layer. *Scr. Mater.* **2014**, *77*, 13−16.

(18) Asad, M.; Li, Q.; Sachdev, M.; Wong, W. S. Thermal and optical properties of high-density GaN micro-LED arrays on flexible substrates. *Nano Energy* **2020**, *73*, 104724.

(19) Luo, X.; Hu, R.; Guo, T.; Zhu, X.; Chen, W.; Mao, Z.; Liu, S. In Low thermal resistance LED light source with vapor chamber coupled fin heat sink. Proceedings from the *60th Electronic Components and Technology Conference (ECTC)*, 1−4 June 2010, Las Vegas, Nevada; IEEE: New York, 1347−1352.

(20) Wan, Z. M.; Liu, J.; Su, K. L.; Hu, X. H.; M, S. S. Flow and heat transfer in porous micro heat sink for thermal management of high power LEDs. *Microelectron. J.* **2011**, *42* (5), 632−637.

(21) Horng, R.; Hong, J.; Tsai, Y.; Wuu, D.; Chen, C.; Chen, C. Optimized Thermal Management From a Chip to a Heat Sink for High-Power GaN-Based Light-Emitting Diodes. *IEEE Trans. Electron Devices* **2010**, *57* (9), 2203−2207.

(22) An, C.; Wu, M.; Huang, Y.; Chen, T.; Chao, C.; Yeh, W. In Study on flip chip assembly of high density micro-LED array. Proceedings from the *6th International Microsystems, Packaging, Assembly and Circuits Technology Conference (IMPACT)*, October 19−21, 2011, Taipei, Taiwan; IEEE: New York, 2011; pp 336−338.

(23) Li, J.; Ma, B.; Wang, R.; Han, L. Study on a cooling system based on thermoelectric cooler for thermal management of high-power LEDs. *Microelectron. Reliab.* **2011**, *51* (12), 2210−2215.

(24) Lai, Y.; Cordero, N.; Barthel, F.; Tebbe, F.; Kuhn, J.; Apfelbeck, R.; Würtenberger, D. Liquid cooling of bright LEDs for automotive applications. *Appl. Therm. Eng.* **2009**, *29* (5), 1239−1244.

(25) Deng, Y.; Liu, J. A liquid metal cooling system for the thermal management of high power LEDs. *Int. Commun. Heat Mass Transfer* **2010**, *37* (7), 788−791.

(26) Niu, S.; Hu, Y.; Wen, X.; Zhou, Y.; Zhang, F.; Lin, L.; Wang, S.; Wang, Z. L. Enhanced performance of flexible ZnO nanowire based room-temperature oxygen sensors by piezotronic effect. *Adv. Mater.* **2013**, *25* (27), 3701−6.
(27) Peng, M.; Li, Z.; Liu, C.; Zheng, Q.; Shi, X.; Song, M.; Zhang, Y.; Du, S.; Zhai, J.; Wang, Z. L. High-resolution dynamic pressure sensor array based on piezo-phototronic effect tuned photoluminescence imaging. *ACS Nano* **2015**, *9* (3), 3143−50.
(28) Zhang, S.; Ma, B.; Zhou, X.; Hua, Q.; Gong, J.; Liu, T.; Cui, X.; Zhu, J.; Guo, W.; Jing, L.; Hu, W.; Wang, Z. L. Strain-controlled power devices as inspired by human reflex. *Nat. Commun.* **2020**, *11* (1), 326.
(29) Peng, Y. Y.; Que, M. L.; Lee, H. E.; Bao, R. R.; Wang, X. D.; Lu, J. F.; Yuan, Z. Q.; Li, X. Y.; Tao, J.; Sun, J. L.; Zhai, J. Y.; Lee, K. J.; Pan, C. F. Achieving high-resolution pressure mapping via flexible GaN/ZnO nanowire LEDs array by piezo-phototronic effect. *Nano Energy* **2019**, *58*, 633−640.
(30) Pan, C. F.; Dong, L.; Zhu, G.; Niu, S. M.; Yu, R. M.; Yang, Q.; Liu, Y.; Wang, Z. L. High-resolution electroluminescent imaging of pressure distribution using a piezoelectric nanowire LED array. *Nat. Photonics* **2013**, *7* (9), 752−758.
(31) Yu, R.; Wu, W.; Pan, C.; Wang, Z.; Ding, Y.; Wang, Z. L. Piezo-phototronic Boolean logic and computation using photon and strain dual-gated nanowire transistors. *Adv. Mater.* **2015**, *27* (5), 940−7.
(32) Wang, X.; Song, W. Z.; You, M. H.; Zhang, J.; Yu, M.; Fan, Z.; Ramakrishna, S.; Long, Y. Z. Bionic Single-Electrode Electronic Skin Unit Based on Piezoelectric Nanogenerator. *ACS Nano* **2018**, *12* (8), 8588−8596.
(33) Yeo, Y. C.; Chong, T. C.; Li, M. F. Electronic band structures and effective-mass parameters of wurtzite GaN and InN. *J. Appl. Phys.* **1998**, *83* (3), 1429−1436.
(34) Wu, W. Z.; Wang, Z. L. Piezotronics and piezo-phototronics for adaptive electronics and optoelectronics. *Nat. Rev. Mater.* **2016**, *1* (7), 16031.
(35) Peng, M.; Zhang, Y.; Liu, Y.; Song, M.; Zhai, J.; Wang, Z. L. Magnetic-mechanical-electrical-optical coupling effects in GaN-based LED/rare-earth terfenol-D structures. *Adv. Mater.* **2014**, *26* (39), 6767−72.
(36) Tsai, S. C.; Lu, C. H.; Liu, C. P. Piezoelectric effect on compensation of the quantum-confined Stark effect in InGaN/GaN multiple quantum wells based green light-emitting diodes. *Nano Energy* **2016**, *28*, 373−379.
(37) BİLGİLİ, A. K.; AKPINAR, Ö.; ÖZTÜRK, M. K.; ÖZÇELİK, S.; ÖZBAY, E. XRD vs Raman for InGaN/GaN structures. *Politeknik Dergisi* **2019**, *23* (2), 291−296.
(38) Kaganer, V. M.; Jenichen, B.; Ramsteiner, M.; Jahn, U.; Hauswald, C.; Grosse, F.; Fernández-Garrido, S.; Brandt, O. Quantitative evaluation of the broadening of x-ray diffraction, Raman, and photoluminescence lines by dislocation-induced strain in heteroepitaxial GaN films. *J. Phys. D: Appl. Phys.* **2015**, *48* (38), 385105.
(39) Cho, Y.-H.; Gainer, G. H.; Fischer, A. J.; Song, J. J.; Keller, S.; Mishra, U. K.; DenBaars, S. P. S-shaped" temperature-dependent emission shift and carrier dynamics in InGaN/GaN multiple quantum wells. *Appl. Phys. Lett.* **1998**, *73* (10), 1370−1372.
(40) Röder, C. Strain, charge carriers, and phonon polaritons in wurtzite GaN-a Raman spectroscopical view. *Ph.D. Thesis*, Freiberg University of Mining and Technology, Freiberg, Germany, 2015.
(41) Koryakin, A. A.; Mizerov, A. M.; Bouravleuv, A. D. On the stress relaxation mechanism of GaN thin films grown on Si(111) substrates. *J. Phys.: Conf. Ser.* **2019**, *1410*, 012046.
(42) Briggs, R. J.; Ramdas, A. K. Piezospectroscopic study of the Raman spectrum of cadmium sulfide. *Phys. Rev. B* **1976**, *13* (12), 5518−5529.
(43) Harima, H. Properties of GaN and related compounds studied by means of Raman scattering. *J. Phys.: Condens. Matter* **2002**, *14* (38), R967−R993.
(44) Wagner, J. M.; Bechstedt, F. Properties of strained wurtzite GaN and AlN: Ab initio studies. *Phys. Rev. B: Condens. Matter Mater. Phys.* **2002**, *66* (11), 115202.
(45) Wang, Z. L. Piezopotential gated nanowire devices: Piezotronics and piezo-phototronics. *Nano Today* **2010**, *5* (6), 540−552.
(46) Takeuchi, T.; Sota, S.; Katsuragawa, M.; Komori, M.; Takeuchi, H.; Amano, H.; Akasaki, I. Quantum-confined stark effect due to piezoelectric fields in GaInN strained quantum wells. *Jpn. J. Appl. Phys. 2* **1997**, *36* (4A), L382−L385.
(47) Hu, Y.; Chang, Y.; Fei, P.; Snyder, R. L.; Wang, Z. L. Designing the electric transport characteristics of ZnO micro/nanowire devices by coupling piezoelectric and photoexcitation effects. *ACS Nano* **2010**, *4* (2), 1234−40.
(48) Jiang, C.; Jing, L.; Huang, X.; Liu, M.; Du, C.; Liu, T.; Pu, X.; Hu, W.; Wang, Z. L. Enhanced Solar Cell Conversion Efficiency of InGaN/GaN Multiple Quantum Wells by Piezo-Phototronic Effect. *ACS Nano* **2017**, *11* (9), 9405−9412.
(49) Huang, X.; Du, C.; Zhou, Y.; Jiang, C.; Pu, X.; Liu, W.; Hu, W.; Chen, H.; Wang, Z. L. Piezo-Phototronic Effect in a Quantum Well Structure. *ACS Nano* **2016**, *10* (5), 5145−52.
(50) Zakgeim, A. L.; Kuryshev, G. L.; Mizerov, M. N.; Polovinkin, V. G.; Rozhansky, I. V.; Chernyakov, A. E. A study of thermal processes in high-power InGaN/GaN flip-chip LEDs by IR thermal imaging microscopy. *Semiconductors* **2010**, *44* (3), 373−379.
(51) Lasance, C. J.; Poppe, A. *Thermal management for LED applications*; Springer, New York, 2014; pp 27−35.
(52) Keppens, A.; Ryckaert, W. R.; Deconinck, G.; Hanselaer, P. High power light-emitting diode junction temperature determination from current-voltage characteristics. *J. Appl. Phys.* **2008**, *104* (9), 093104.
(53) Peter, Y.; Cardona, M. In *Fundamentals of semiconductors: physics and materials properties*; Springer-Verlag: Berlin, 2010; pp 1−15.
(54) Masui, H.; Kroemer, H.; Schmidt, M. C.; Kim, K.-C.; Fellows, N. N.; Nakamura, S.; DenBaars, S. P. Electroluminescence efficiency of $(10\bar{1}0)$-oriented InGaN-based light-emitting diodes at low temperature. *J. Phys. D: Appl. Phys.* **2008**, *41* (8), 082001.
(55) Lee, H. K.; Yu, J. S.; Lee, Y. T. Thermal analysis and characterization of the effect of substrate thinning on the peformances of GaN-based light emitting diodes. *Phys. Status Solidi A* **2010**, *207* (6), 1497−1504.
(56) Guo, X.; Schubert, E. F. Current crowding and optical saturation effects in GaInN/GaN light-emitting diodes grown on insulating substrates. *Appl. Phys. Lett.* **2001**, *78* (21), 3337−3339.
(57) Shchekin, O. B.; Epler, J. E.; Trottier, T. A.; Margalith, T.; Steigerwald, D. A.; Holcomb, M. O.; Martin, P. S.; Krames, M. R. High performance thin-film flip-chip InGaN-GaN light-emitting diodes. *Appl. Phys. Lett.* **2006**, *89* (7), 071109.
(58) Ding, J.; Che, L. J.; Chen, X.; Zhang, T.; Huang, Y. D.; Huang, Z. L.; Zeng, Z. M.; Zhang, H. L.; Ding, S. N.; Yang, H. Interdigital Structure Enhanced the Current Spreading and Light Output Power of GaN-Based Light Emitting Diodes. *IEEE Access* **2020**, *8*, 105972−105979.
(59) Sze, S. M.; Ng, K. K., LEDs and Lasers. In *Physics of Semiconductor Devices*; Wiley: 2006; pp 599−662.
(60) Keppens, A.; Ryckaert, W. R.; Deconinck, G.; Hanselaer, P. Modeling high power light-emitting diode spectra and their variation with junction temperature. *J. Appl. Phys.* **2010**, *108* (4), 043104−043104.
(61) Schubert, E. F. Theory of radiative recombination. In *Light-Emitting Diodes*, 2nd ed.; Cambridge University Press: Cambridge, 2006; pp 48−58.
(62) Wang, T. H.; Xu, J. L.; Wang, X. D. The effect of multi-quantum barrier structure on light-emitting diodes performance by a non-isothermal model. *Chin. Sci. Bull.* **2012**, *57* (30), 3937−3942.
(63) Kim, D. S.; Han, B. Effect of junction temperature on heat dissipation of high power light emitting diodes. *J. Appl. Phys.* **2016**, *119* (12), 125104.

https://doi.org/10.1021/acs.nanolett.1c00999
Nano Lett. XXXX, XXX, XXX−XXX

(64) Hader, J.; Moloney, J. V.; Koch, S. W. Supression of carrier recombination in semiconductor lasers by phase-space filling. *Appl. Phys. Lett.* **2005**, *87* (20), 201112.

https://doi.org/10.1021/acs.nanolett.1c00999
Nano Lett. XXXX, XXX, XXX−XXX